

BIOSORPTION OF LEAD HEAVY METAL ON PRICKLY PEAR CACTUS BIOMATERIAL: KINETIC, THERMODYNAMIC AND REGENERATION STUDIES

HANEN NOURI, ASMA ABDEDAYEM, INES HAMIDI, SOUAD SOUISSI NAJJAR and
ABDELMOTTALEB OUEDERNI

*Research Laboratory of Process Engineering and Industrial Systems, National School of Engineers of
Gabes, University of Gabes, Omar Ibn El Khattab Str., 6029 Gabes, Tunisia*

✉ *Corresponding author: H. Nouri, hanennouri@gmail.com*

Received April 27, 2021

The potential of Tunisian prickly pear cactus as a low-cost adsorbent for Pb(II) ions from aqueous solution was investigated in batch mode. To determine the optimum adsorption conditions, experiments were conducted varying the operating parameters, as follows: pH of the solutions (2-10), initial concentration of metal ions (0.98-2.4 mmol/L) and temperature (30-60 °C). The adsorption isotherm data were analyzed by applying the Langmuir, Freundlich, Dubinin–Raduskevich, Temkin and Redlich–Peterson models. The experimental results were better fitted by the Freundlich model. The pseudo-first order, pseudo-second order, Elovich and intraparticle diffusion models were applied to the description of the kinetic data. The best fit was achieved for the pseudo-second order model, and the presence of both film and intraparticle diffusion mechanisms was demonstrated. Thermodynamic studies indicated that the biosorption on the cladode powder is an exothermic and chemical process. The desorption/regeneration process was also investigated. The obtained results revealed over 90% desorption of Pb(II) metal ions from the total metal-loaded mass of the adsorbent and good stability of the cactus adsorbent for four successive adsorption/desorption cycles.

Keywords: prickly pear cactus, biosorption, lead, thermodynamic, kinetic, regeneration

INTRODUCTION

The environment is seriously endangered by the large amounts of heavy metals discharged into water bodies every year caused by human activities.¹⁻³ Heavy metals represent the most common environmental pollutants. Several metals, such as cadmium, lead, copper, mercury, chromium, manganese, *etc.*, are known to be highly toxic.⁴ Particularly, lead is very toxic, even in very low concentrations, and has destructive effects on the environment and human health.^{4,5} The World Health Organization⁶ affirms that the highest permitted concentration value of lead in water sources is about 0.01 mg/L. This concentration value is the threshold to be respected for protection of human health and the environment, as well as for the preservation of an ecological equilibrium.⁶ Therefore, contamination of water bodies by trace metals has become an issue of global concern, while the demand for metal recovery is a major challenge.⁷

The level of such toxic contaminants as Pb in wastewater must be reduced, while the heavy metal should be recycled, if possible. Therefore, various strategies and processes have been developed for the removal of lead from discharged wastewater, such as chemical precipitation, electrodialysis, reverse osmosis, solvent extraction, ion exchange, coagulation and membrane separation.^{3,8,9} Nevertheless, these conventional techniques are no longer used because they have proved inadequate, unsuccessful or expensive to apply.¹⁰⁻¹² Moreover, these techniques showed low efficiency, especially for the removal of low concentrations of heavy metal ions from wastewaters. In recent years, the adsorption process has attained significant attention, considering its simplicity, low cost and high efficiency in the recovery of metals from aqueous solutions. The economic feasibility of the adsorption technique has been enhanced by using biomaterials as a promising alternative to conventional adsorbents, such as activated carbon, which is well-known as a useful adsorbent for heavy metals.¹³ In addition, the use of plant materials (biosorbents) is encouraged due to many advantages: their abundance in nature, high efficiency of the adsorbent, and minimum chemical and biological sludge production, which makes their regeneration possible, without secondary pollution.^{13,14} Thus, several plant-based adsorbents have been investigated in order to determine their

maximum sorption uptake and lead affinity, such as maize stover,⁸ *Landoltia punctata* and *Spirodela polyrhiza*,¹⁵ *Opuntia streptacantha*,¹⁶ *Mansonina* wood sawdust,¹⁷ algae, bacteria and fungi.³

The prickly pear cactus is an inexpensive and abundant plant in several developing countries. In Tunisia, the cactus production area was around 450000 hectares in 2002, as presented by the FAO.¹⁸ Cactus has been interestingly assessed as an adsorbent for metals removal. Several research works suggested that this plant (cladodes, fruit, and peels) has a great potential for the treatment of water, in particular, for the elimination of turbidity, biosorption of heavy metals or organic species (dyes, pesticides).¹⁹ Remarkably, Ahrha *et al.* proved that the adsorption capacity of cactus cladode for Pb elimination can reach 62.9 mg/g, compared to 21.6 mg/g for Zn adsorption.²⁰ Similarly, Barka *et al.* indicated that the adsorption capacities of dried cactus cladode for Pb and Cd were 98.62 mg/g and 30.42 mg/g, respectively.⁹ Fernandez-Lopez *et al.*²¹ proved that the removal rate of Cr(VI) from water using *Opuntia ficus-indica* cactus can reach 80%. Interestingly, the highest removal level of 36% for Mn from aqueous solution was obtained using dried cactus peels.²² Derbe *et al.*²³ also investigated the removal of Pb and Cd using cactus powder. Important removal rates, of 58% and 46%, respectively, for Pb and Cd were obtained.

Considering existing reported results, the prickly pear cactus can be a promising biosorbent for various pollutants. Hence, the aim of the present study has been to exploit the potential of this abundant plant in Tunisia for wastewater remediation, investigating dried cactus cladode powder as an environmentally friendly adsorbent for the removal of Pb²⁺ from aqueous solutions. Its Pb(II) removal efficiency was studied varying the experimental conditions, namely, initial solution pH, contact time and temperature. To understand the biosorption process, the kinetics of Pb²⁺ adsorption onto dried cactus was examined and adsorption models were used to fit the experimental data. Finally, the possibility to valorise the spent cactus adsorbent loaded with metal ions, by its regeneration, was also analysed, in order to find the best way to minimize the problem of exhausted biosorbents.

EXPERIMENTAL

Biosorbent preparation

Prickly pear cactus cladodes were collected from the region of Mareth (Gabes) in Tunisia. The collected biomaterial was then peeled and washed with distilled water to remove impurities. Then, they were dried in an oven at 60 °C for 48 h. The dried cladodes were sieved to a particle size in the range of 0.2-1.2 mm. The obtained biosorbent was stored for further use without any pretreatment.

Batch adsorption experiments

A Pb(II) stock solution (500 mg/L) was prepared by dissolving an appropriate amount of Pb(CH₃COO)₂·7H₂O in ultrapure deionized water (UP water). The pH was adjusted to a given value by addition of HCl or NaOH solutions.

Biosorption experiments were conducted in 100 mL glass flasks at a constant agitation speed. The experiments were carried out by varying the biosorbent mass (0.05-10 g/L). The equilibrium time was set as 24 h, which was enough to reach the equilibrium of adsorption according to preliminary tests. The effect of temperature was studied in the range of 30-60 °C. After each biosorption procedure completed, the samples were filtered through a 0.45-μm syringe filter. The Pb concentration in the solutions was determined using Inducted Coupled Plasma (ICP-AES) spectrometry (HORIBA JOBIN YVON). A calibration curve was determined in the concentration range of 0 to 50 mg/L, at the wavelength of 283 nm, according to the standard solution of Pb. During analysis, the concentration was measured three times to insure the obtained values.

The amount of Pb uptake at equilibrium, q_e (mg/g), was determined using the mass balance equation, as follows:

$$q_e = \frac{(C_0 - C_e)}{m} \times V \quad (1)$$

where C_0 (mg/L) is the initial Pb(II) concentration in the solution, C_e (mg/L) is the Pb(II) concentration in the solution at equilibrium, m (g) is the mass of the dried cactus cladode, and V (L) is the volume of the Pb(II) solution.

Biosorbent characterization

The point of zero charge was determined according to the method described by Lopez-Ramon *et al.*²⁴ The pH_{pzc} is the pH at which the amount of negative charges on the adsorbent surface is equal to the amount of positive charges.²⁵ Dried cactus (0.15 mg) was suspended in 50 mL of NaCl solution (0.1 M). The initial pH of the solution was adjusted to defined values from 2.0 to 12.0, using HCl and NaOH solutions. The suspension

was sealed and allowed to equilibrate at 25 °C for 48 h. After this period, the pH of the solution (pH_f) was measured. pH_{pzc} was derived from the curve pH_f = f(pH_i).

FTIR analysis was employed to identify the different functional groups on the surface of the cactus cladodes, which may be responsible for metal binding.

The iodine number of the cactus powder was also determined using the iodine analysis method.²⁶ 1 g of cactus powder was added to an HCl solution (0.1 N), then 100 mL of iodine solution (0.1 N) was also added. After filtration, the filtrate was titrated using a thiosulfate solution of 0.1 N. The corresponding iodine number was calculated using Equation (2):

$$NI = \frac{(12693 \times N_1 - (279.18 \times N_2 \times v)) \times D}{m} \quad (2)$$

where N₁: normality of iodine solution (N), N₂: normality of thiosulfate solution (N), D: correction factor obtained from the correspondent concentration of the iodine solution, m: mass of cactus (g), V: volume of the solution (mL).

The residual concentration of iodine in the solution is given by the following equation:

$$C = \frac{N_2 \times v}{50} \quad (3)$$

where C: the residual concentration of iodine (N).

In addition, the methylene blue number of the adsorbent was also analyzed. 1 g of cactus powder was put in contact with an MB solution during 24 h. After filtration, the residual concentration of MB was determined using UV-VIS analysis at the wavelength at 664 nm.

The methylene blue number was determined by the following equation:

$$N_{MB} = \frac{C_{MB_0} - C_{MB}}{m} \times V \quad (4)$$

Modeling of adsorption isotherms

The equilibrium adsorption isotherm of lead on prickly pear cactus was analyzed using different isotherm models: Langmuir, Freundlich, Dubinin–Raduskevich, Redlich–Peterson and Temkin.

The Langmuir model²⁷ is based on the assumptions of a homogeneous adsorbent surface with identical adsorption sites,²⁸ and at the maximum adsorption only a monolayer is formed. This model is described by the following equation:

$$Q_{ads} = Q_{max} \cdot \frac{K_L C_e}{1 + K_L C_e} \quad (5)$$

where Q_{ads} is the quantity adsorbed per gram of solid at the equilibrium (mg/g), Q_{max} is the saturation adsorption capacity (mg/g), C_e (mg/L) is the equilibrium concentration of the adsorbate and K_L is the affinity constant or Langmuir constant (L/mg).

The Freundlich isotherm is an empirical equation that assumes heterogeneous distribution of adsorptive energies on the adsorbent surface. It can be employed to describe multilayer sorption and can be written as follows:²⁹

$$Q_{ads} = K_f C_e^{\frac{1}{n}} \quad (6)$$

where Q_{ads} (mg/g) is the amount of adsorbate adsorbed per gram of adsorbent at equilibrium, C (mg/L) is the equilibrium concentration of adsorbate in the solution, K_F ((mg/L)(L/g)^{1/n}) is related to the adsorption capacity, and 1/n gives an idea about the adsorption affinity and heterogeneity of the surface of the adsorbent. When 1/n is small, the adsorption affinity increases,³⁰ while when 1/n is high the heterogeneity of the adsorbent surface is enhanced.³¹

The Temkin isotherm model describes the effect of some indirect adsorbate/sorbate interactions and suggests that the adsorption heat of all the molecules in the layer would linearly decrease with coverage.³² It has been generally applied in the following form:

$$Q_e = B \ln A + B \ln C_e \quad (7)$$

where B is the Temkin constant related to the heat of sorption (J mol⁻¹), A is the Temkin isotherm constant (L/g).

The Dubinin–Raduskevich model was applied to identify if adsorption occurred by a physical or chemical process.³³ The D–R equation is described by the following equation:

$$Q_e = Q_m e^{\left(-k \cdot \varepsilon^2\right)} \quad (8)$$

where k is a constant related to the adsorption energy (mol² kJ⁻²), ε is the Polanyi potential calculated from the following equation:

$$\varepsilon = RT \cdot \ln \left(1 + \frac{1}{C_e} \right) \quad (9)$$

The Redlich–Peterson model is a combination of the Langmuir and Freundlich equations into a single one. It proposes an empirical equation, which may be used to represent adsorption equilibrium over a wide concentration range in either heterogeneous or homogenous systems.³⁴ At low surface coverage, the Redlich–Peterson equation reduces to the Freundlich isotherm at high adsorbate concentration, and to the Langmuir isotherm when $\beta = 1$. The equation is given as:

$$Q_e = \frac{K_R C_e}{1 + \alpha_R C_e^\beta} \quad (10)$$

where K_R is the Redlich–Peterson isotherm constant ($\text{L} \cdot \text{g}^{-1}$), α_R is Redlich–Peterson isotherm constant ($\text{L} \cdot \text{mg}^{-1}$), β is the exponent, which lies between 0 and 1.

Modeling of adsorption kinetics

Several models are used to investigate the adsorption process. In the present study, the pseudo-first order, pseudo-second order, and Elovich models were used to fit the experimental data.

The pseudo-first order model, also known as Lagergren model, describes the adsorption in solid/liquid systems based on the adsorption capacity of the solid. It assumes that a metal ion is adsorbed on one site of adsorbent.³⁵ This model can be written in the linear form as follows, with respect to the boundary conditions $q = 0$ at $t = 0$ and $q = q_e$ at $t = t$:^{36,37}

$$\ln(q_e - q) = \ln(q_e) - k_1 t \quad (11)$$

where q_e and q_t are the adsorbed amounts of the solute (mmol/g or mg/g) at equilibrium and at time t (min), and k_1 is pseudo-first order rate constant (min^{-1}).

The pseudo-second order model is based on the assumption that the rate limiting step is the surface adsorption that involves chemisorption, where the removal from a solution is due to physicochemical interactions between the adsorbate and the adsorbent.

The linear expression of the pseudo-second order model is presented as follows:³⁶

$$\frac{t}{q_t} = \frac{1}{k_2 q_e^2} + \frac{1}{q_e} t \quad (12)$$

where q_e and q_t are the adsorption capacity at equilibrium and at time t (min), respectively (mmol/g), and k_2 is the rate constant ($\text{g/mmol} \cdot \text{min}$).

The simplified Elovich or Roginsky–Zeldovich equation, obtained by Chien and Clayton (1980)³² for $\alpha\beta t \gg 1$, by applying the boundary conditions $q_t = 0$ at $t = 0$ and $q_t = q_e$ at $t = t$, is expressed as follows:^{37,38}

$$q_t = \beta \ln(\alpha\beta) + \beta \ln(t) \quad (13)$$

where q_t is the amount of adsorbed species at time t , α is the initial metal ion adsorption rate ($\text{mmol}/(\text{g} \cdot \text{min})$) and β is the desorption constant (g/mmol).

RESULTS AND DISCUSSION

Biosorbent characterization

The analysis of the pH_{pzc} gives information about the acidic or basic character of the used material, as well as the net surface charge of the material, knowing the pH of the solution. Therefore, to know the behavior of the prickly pear cactus biosorbent, the pH_{pzc} before the adsorption step was determined. The results are shown in Table 1.

The obtained results indicate that the virgin prickly pear cactus presents neutral to basic pH_{pzc} . The pH_{pzc} of the cactus implies that the adsorption of Pb(II) ions will be favored at higher pH values above 7.

Iodine and methylene blue numbers were determined. The corresponding values are summarized in Table 1. As can be seen, the cactus cladode adsorbent presents an important iodine number compared to other biomaterials. This can suggest the porosity of this type of biomass. In addition, the high methylene blue number of the cactus proves its ability to adsorb macro-organic molecules. Both numbers indicate that the cactus surface presents a large distribution of pores, especially macropores. These characteristics can favor the adsorption of lead onto its surface.

The infrared spectra ($400\text{--}4000 \text{ cm}^{-1}$) of the cactus powder, before and after adsorption, are shown in Figure 1. The spectra of both the raw cactus and the Pb loaded cactus show broad overlapping bands in the $3900\text{--}3200 \text{ cm}^{-1}$ region, which are due to the elongation of O-H bonds. The band at

2923.8 cm^{-1} and the band at 2846.7 cm^{-1} correspond, respectively, to the vibrations of asymmetric elongation of CH_2 and the symmetrical elongation of $-\text{CH}_3$ of aliphatic acids.³⁹ The presence of the band at 1617 cm^{-1} indicates the presence of the carboxyl groups. The 1319.2 cm^{-1} band comes from the vibrating strain of the $-\text{OH}$ groups of phenolic compounds. The peaks observed at 1370.45 cm^{-1} reflect the vibrations of symmetrical or asymmetric valence of the carboxylic groups of the pectin.⁴⁰ The band at 1026 cm^{-1} could be assigned to the vibration of the C-O-C or $-\text{OH}$ groups and the polysaccharides.⁴¹ The absorption peaks in the region of wavenumbers below 800 cm^{-1} can be attributed to nitrogenous bioligands.⁴² In addition, spectral analysis after Pb(II) biosorption showed that there was a substantial decrease in the wavenumber of carboxylic acid groups at 1617 cm^{-1} and 1370 cm^{-1} . This indicates that carboxylic acid groups were likely responsible for binding Pb(II) onto the dried cactus biosorbent. The groups of C-OH, and C-O-C were also involved in Pb(II) binding to some extent.⁹

Table 1
Characterization of cactus biosorbent

pH_{pzc}	Iodine number (mg/g)	Methylene blue number (mg/g)
7.2	196	400

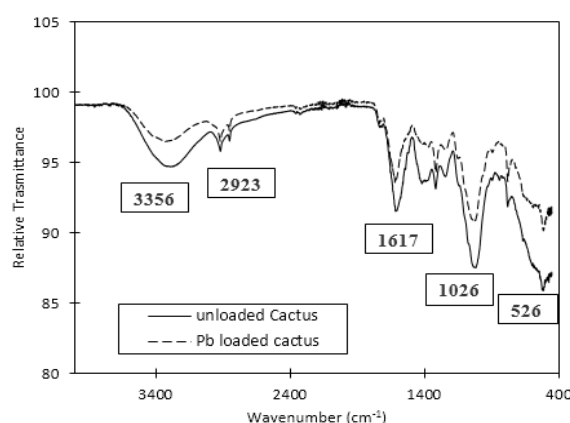


Figure 1: FTIR spectra of unloaded and Pb-loaded cactus biosorbent

Effect of pH

The pH of the solution is one of the main parameters controlling the biosorption process, which influence both metal solubility and biosorbent surface charge.²⁵ The removal of Pb(II) was studied at 30 °C at 5 g/L of biosorbent amount and 2.4 mmol/L of metal initial concentration, while varying the pH from 2 to 10. Figure 2 shows the effect of pH on the removal of Pb(II) ions. The result indicates that the adsorption of Pb(II) is strongly affected by the pH of the medium. The adsorption was low in acidic medium, but increased with the rising pH of the solution. The percentage adsorbed increased from 34% to 80% when the pH was increased from 2.0 to 10. According to the pH_{pzc} value of the cactus, at lower pH values, the biosorption of Pb(II) is low because large quantities of protons compete with metal cations for adsorption sites on the biomass surface. As the pH increased, the number of positively charged available sites decreased and the number of negatively charged sites increased. Thus, the surface of the biosorbent became negatively charged, and this increased the biosorption of the positively charged metal ions through electrostatic forces of attraction. Similar results were found by Barka *et al.*⁹ for the biosorption of Cd(II) and Pb(II) onto cactus.

The decrease in the fixation of lead for pH values higher than 8 is caused by the complexation of lead ions by OH^- groups, which would prevent metal biosorption.⁹

Effect of biosorbent particle size

The particle size is considered an important parameter that affects the kinetics of adsorption, determining the diffusion of solute onto the adsorbent particles.

The kinetics of Pb(II) biosorption was examined for different particle sizes of dried cactus (0.2-0.6 mm, 0.6-1 mm, 1-1.6 mm and over 1.6 mm). The results presented in Figure 3 show that the adsorbed

amount of metal ions increases exponentially over time until it reaches the equilibrium in all conditions. In addition, the decrease in particle size led to an increase in lead removal. For the smaller particle size, of 0.2-0.6 mm, the equilibrium was reached in 50 min. However, for particles with a diameter larger than 1.6 mm, the equilibrium was obtained in almost 100 min.

In fact, the higher adsorption kinetics achieved by the smaller size of biosorbent may be explained by the greater accessibility of lead to cactus pores. This can suggest the existence of internal mass transfer resistance.

Effect of stirring speed

Stirring speed is an important parameter that influences the adsorption kinetics and could prove the existence or absence of external mass transfer resistance. Kinetic experiments were conducted for different stirring speeds, an initial ion concentration of 500 mg/L, pH = 5, T = 30 °C and particle size = 1-1.6 mm. The obtained results are illustrated in Figure 4. The adsorption process was found to be fast in the first 20 minutes, then it slowed down until it stagnated at the equilibrium stage. The adsorption capacity was found to increase with the stirring speed. In fact, the amount of lead adsorbed at equilibrium increased from 55 to 70 mg/g when the stirring speed increased from 100 to 500 rpm. This result proves the existence of external mass transfer limitation, which decreases with the stirring speed and then enhances the adsorption capacity.

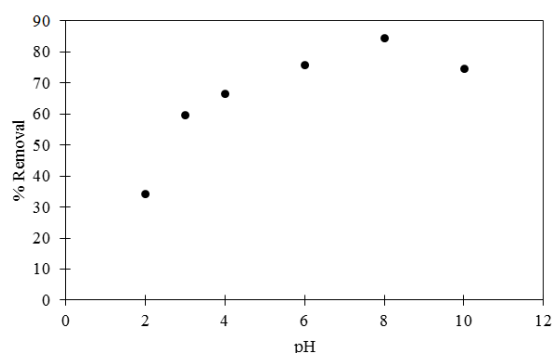


Figure 2: Effect of pH on adsorption of Pb(II) ions onto the cactus biomaterial (T: 30 °C, C: 2.4 mmol/L, m: 4 g/L)

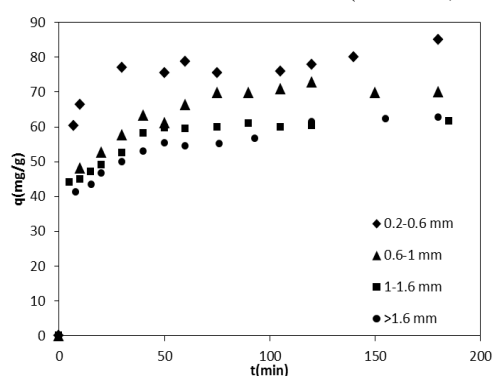


Figure 3: Effect of biosorbent particle size on lead adsorption capacity ($C_0 = 500$ mg/L, T = 30 °C, pH 5, m = 4 g/L, stirring speed = 300 rpm)

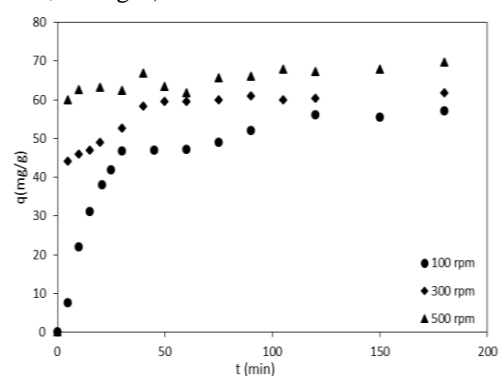


Figure 4: Effect of stirring speed on lead adsorption capacity ($C_0 = 500$ mg/L, T = 30 °C, pH 5, m = 4 g/L, particle size = 1-1.6 mm)

Table 2
Adsorption isotherm parameters of Pb(II) removal by the cactus cladode biosorbent

Model	Temperature (°C)	30	40	50	60
Langmuir	Q_{\max} (mg/g)	714.28	156.25	71.44	79.36
	K_L (L/mg)	0.0013	0.0020	0.0035	0.0019
	R^2	0.985	0.962	0.877	0.797
Freundlich	K_f	2.285	0.016	0.003	0.00033
	$((\text{mg/L})(\text{L/g})^{1/n})$				
	n	1.37	0.617	0.568	0.47
Temkin	R^2	0.960	0.971	0.993	0.992
	A (L/g)	0.035	0.017	0.011	0.01
	B (J mol ⁻¹)	73.16	75.65	55.14	39.33
Dubinin–Radushkevich	R^2	0.973	0.744	0.774	0.563
	Q_m (mg/g)	224.17	623.96	423.63	171.92
	K (g ² kJ ⁻²)	0.34	0.154	0.184	0.135
Redlich–Peterson	R^2	0.982	0.962	0.866	0.825
	α_R (L mg ⁻¹)	7.74E-07	0	5.04E-02	5.09E-02
	β	2.42	0.901	0	0
	R^2	0.959	0.826	0.69	0.926

Adsorption isotherm

The adsorption isotherm given by the equilibrium data provides the basic parameters for the design of adsorption systems, revealing the amount of adsorbent required to remove a pollutant mass under the system conditions.²⁵ The Langmuir, Freundlich, Temkin, Dubinin–Radushkevich and Redlich–Peterson isotherm models were applied to the analysis of the equilibrium sorption data. The results are shown in Table 2.

From the values of the correlation coefficient (R^2) of different models shown in Table 2, it can be noticed that all the models provide a good fit to the experimental data. However, the Freundlich model is the most suitable one, fitting the experimental data for all experimental conditions (temperature and pH). Thus, it will be considered for the description in the rest of the study. The value of n (Freundlich constant) lies between 1 and 10, indicating favorable adsorption of Pb onto the surface of the cactus biosorbent.²⁵

Thermodynamic study

The evolution of Pb biosorption onto dried cactus as a function of temperature is shown in Figure 5. It was observed that the biosorption dramatically decreased as the temperature increased from 30 °C to 60 °C, which indicates that low temperature favors Pb(II) biosorption. In general, the temperature presents two main effects on the biosorption process. Increasing the temperature is commonly used to increase the rate of diffusion of the biosorbed molecules across the external boundary layer and the internal pores of the biosorbent particles, owing to the decrease in the viscosity of the solution. In addition, modifying the temperature will change the equilibrium capacity of the biosorbent for the adsorbate.^{9,25}

The observed trend may be due to the tendency of Pb(II) ions to escape from the solid phase to the bulk phase with an increase in the temperature of the solution.

In order to examine the feasibility of the adsorption process, thermodynamic parameters, such as the standard free energy (ΔG^0), enthalpy change (ΔH^0) and entropy change (ΔS^0), were estimated. The Gibbs free energy change of Pb (II) adsorption was calculated using the following equation:⁴³

$$\Delta G^0 = -RT \ln(K_D) \quad (14)$$

$$K_D = \frac{q_e}{C_e} \quad (15)$$

The Gibbs free energy is also related to the enthalpy change and entropy change at constant temperature by the Van't Hoff equation as follows:

$$\Delta G^0 = \Delta H^0 - T \Delta S^0 \quad (16)$$

The values of ΔH^0 and ΔS^0 were calculated from the slope and intercept of the plot of $\ln(K_D)$ versus $1/T$ and the thermodynamic parameters are listed in Table 3.

At a low temperature of 30 °C, the negative values of ΔG^0 obtained indicate that the adsorption process onto the cactus surface is spontaneous in nature. However, after increasing the temperature, the ΔG^0 turns to positive values, indicating a non-spontaneous process. This confirms that increasing temperature is not favorable for Pb adsorption onto the cactus surface, showing that the biosorption is based on a chemical mechanism. This explains the reason why the kinetic data did not fit the pseudo-first order model (a physisorption model).

The magnitude of ΔH^0 gives information about the type of adsorption. From Table 3, the value of ΔH^0 obtained indicates that the biosorption of Pb(II) ions is an exothermic process.

Furthermore, the negative value of ΔS^0 indicates a decrease in randomness at the solid/solution interface during adsorption.

Kinetic study

The kinetic experiments were performed using 4 g/L of cladode powder, with a particle diameter between 0.2-0.6 mm, and initial lead concentrations of 2.4, 0.96 and 0.24 mmol/L.

The biosorption process was found to be rapid and reached equilibrium in 30 min, with adsorption efficiency between 70 and 90% (Fig. 6). Then, the rate of biosorption became slower and stagnated with the increase in contact time.

Linear regression analysis (coefficient of determination R^2) was used to analyze the linear forms of each kinetic model. Kinetic constants were determined using the slope and intercept values of the linear plots. The obtained data are given in Table 4.

Table 3
Thermodynamic parameters of Pb(II) adsorption onto the cactus cladode biosorbent

T (°K)	$\ln(K_D)$	ΔH^0 (kJ/mol)	ΔS^0 (J/mol K)	ΔG^0 (kJ/mol)
303	0.142	-44.17	-145.73	-0.0134
313	-0.632			1.443
323	-1.360			2.901
333	-1.355			4.358

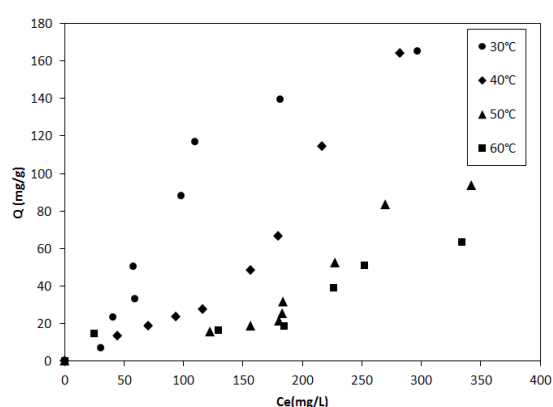


Figure 5: Effect of temperature on Pb(II) adsorption onto the cactus cladode biomaterial (pH: 5, C: 500 mg/L)

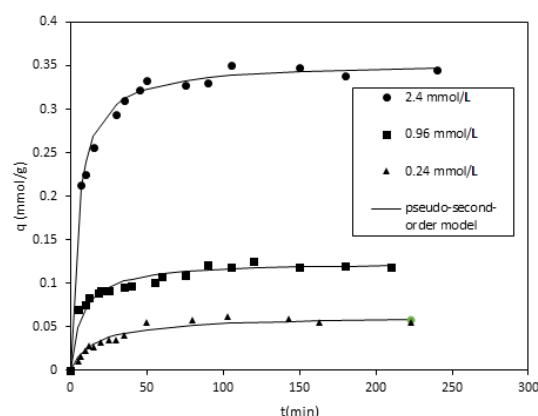


Figure 6: Effect of initial metal ion concentration on Pb(II) adsorption onto the cactus cladode biomaterial (m: 4 g/L, T: 30 °C, pH 5)

Table 4
Kinetic parameters of different models for the adsorption of Pb(II) onto cactus cladode powder

C ₀ (mmol/L)	q _{exp} (mmol/g)	Pseudo-first order			Pseudo-second order			Elovich			
		k ₁ (min ⁻¹)	q _{e cal} (mmol/g)	R ²	k ₂ (g/mmol.min)	q _{e cal} (mmol/g)	R ²	α (mmol/(g.min))	B (g/mmol)	q _{e cal} (mmol/g)	R ²
2.413	0.343	0.055	0.210	0.964	0.591	0.354	0.999	1161.69	0.04	0.36	0.878
0.965	0.118	0.022	0.048	0.927	1.043	0.124	0.997	1166.14	0.015	0.12	0.941
0.241	0.055	0.031	0.047	0.940	0.987	0.062	0.987	39.07	0.013	0.06	0.912

Table 4 shows that the correlation coefficients for the pseudo-first order and Elovich models are very low and the predicted values of q_{ecal} were not reasonably close to the experimental q_e values, suggesting their insufficiency to fit the kinetic data. The correlation coefficients for the pseudo-second order kinetic model are nearly equal to 1, and the predicted values of q_e are comparable to the experimental ones. This model was found more suitable to the description of the kinetics of heavy metal ions adsorbed onto different materials.⁴⁴ Barka *et al.* suggest that the biosorption of Pb(II) onto dried cactus is presumably a chemisorption process, involving an exchange between metal ions and the functional groups of the biosorbent.⁹

Mechanism of biosorption

The overall adsorption process may be controlled by either one or more steps, *e.g.*, film or external diffusion, pore diffusion, surface diffusion and adsorption on the pore surface, or a combination of these. The possibility of intraparticle diffusion was explored by using the intraparticle diffusion model proposed by Weber and Morris,⁴⁵ presented by the following equation:

$$q_t = k_p t^{1/2} + C \quad (17)$$

where k_p (mol/g.min^{1/2}) is the intraparticle diffusion rate constant and C is a constant of the model that can give an idea about the thickness of the boundary layer, the larger the value of C , the more effective is the boundary layer.

If the Weber–Morris plot of q_t versus $t^{1/2}$ satisfies the linear relationship with the experimental data, then the sorption process is controlled by intraparticle diffusion only. However, if the data show multi-linear plots, then two or more steps influence the sorption process.⁹

The plot of q_t versus $t^{1/2}$ for the adsorption of Pb(II) at three metal ion concentrations is depicted in Figure 7. It is clear that this curve shows three distinct steps: external diffusion, intraparticle diffusion and the equilibrium stage. The first slope covering the time range between 0-15 min must be external diffusion. This is related to the diffusion of metal ions through the solution to the active sites distributed on the outer surface of the cactus cladode. The second linear portion corresponding to the adsorption period of 15-60 min is assigned to intraparticle diffusion. The third linear portion corresponding to the time of 60-300 min represents the establishment of the equilibrium.

A decrease in the slope (which is equal to k_p) of each segment was observed. Barka *et al.* explained it by the reduction in pore size. In fact, as pore size decreases, the path available for diffusion becomes smaller, which leads to a decrease in the rate of diffusion.⁹ This kind of multi-linearity in the shape of the intraparticle diffusion plot has also been observed in the biosorption of lead onto *Mansonia* wood sawdust¹⁶ and the adsorption of heavy metals onto activated carbon from olive stones.⁴⁶

The values of the correlation coefficients and the diffusion rate constants kp_1 and kp_2 , respectively, of the external and the intraparticle diffusion are presented in Table 5. This table shows that kp_1 values are higher than kp_2 . The boundary layer thickness C and kp_1 increase with the increase of Pb concentration, indicating that the adsorption process was more rapid for high concentrations, providing better driving force for the external mass transfer process. kp_2 values did not show any definite trend with increasing ion concentration.

Furthermore, to identify whether external or intraparticle diffusion is the limiting step that controls the lead adsorption, we calculated the film diffusion coefficient D_f and pore diffusion coefficient D_p using Boyd's model based on the Fick's law. The relationship between the fractional approach to equilibrium (q_t/q_e) and the uptake time is given by:⁴⁷

$$\frac{q_t}{q_e} = 6\left(\frac{Dt}{r^2}\right)^{0.5} \left\{ \pi^{-0.5} + 2 \sum_{n=1}^{\infty} \text{ierfc} \frac{nr}{Dt^{0.5}} \right\} - 3 \frac{Dt}{r^2} \quad (18)$$

For short times, D is replaced by D_f and Equation (18) is simplified as follows:

$$\frac{q_t}{q_e} = 6\left(\frac{D_f}{\pi r^2}\right)^{0.5} t^{0.5} \quad (19)$$

where q_t and q_e are lead uptake (mmol/g) at time t and at equilibrium, respectively, r is the radius of adsorbent particles assumed to be spherical, D_f is the film diffusion coefficient (cm²/s) determined from the slope of the plot of q_t/q_e versus $t^{0.5}$.

As t tends to a higher value, the above equation can be written as follows:

$$\frac{q_t}{q_e} = 1 - \frac{6}{\pi^2} \exp(-Bt) \quad (20)$$

$$\text{and } B = \frac{D_p \pi^2}{r^2} \quad (21)$$

If the plot of B versus t is linear and passes through the origin, then intraparticle diffusion controls the adsorption rate, otherwise it is controlled by film diffusion. All the plots obtained in Figure 8 are linear and do not pass through the origin, indicating film diffusion.

The slopes (B) of the plots of B versus t, at different initial Pb(II) concentrations, were used to calculate the pore diffusion coefficient. The values of external and pore diffusion coefficients are illustrated in Table 5. The data show that these coefficients decrease with increasing metal ion concentrations. This decrease can be justified by the decrease in free active adsorbent sites that cannot meet the excess of metal ion concentrations in solutions. A similar observation was also reported in the literature.^{46,47}

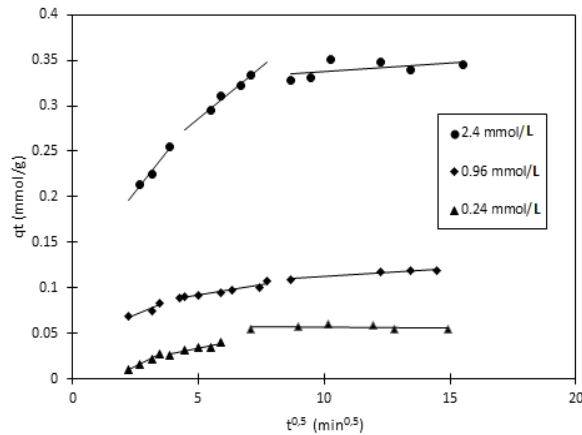


Figure 7: Intraparticle diffusion plots for Pb(II) adsorption onto cactus cladode for different initial ion concentrations (m: 4 g/L, T: 30 °C, pH 5)

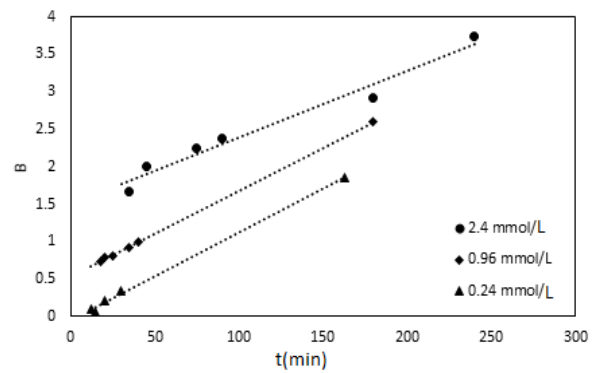


Figure 8: B versus t plots for Pb(II) adsorption onto dried cactus cladode powder

Table 5

Calculated kinetic parameters of intraparticle diffusion model for Pb(II) adsorption onto cactus cladode powder

C_0 (mmol/L)	Intraparticle diffusion model						Film diffusion	Pore diffusion
	First step			Second step			$10^6 \cdot D_f$ (cm^2/s)	$10^6 \cdot D_p$ (cm^2/s)
	kp_1 ($\text{mmol} \cdot \text{min}^{-0.5} \cdot \text{g}^{-1}$)	C	R^2	kp_2 ($\text{mmol} \cdot \text{min}^{-0.5} \cdot \text{g}^{-1}$)	C	R^2		
0.24	0.014	-0.021	0.995	0.006	0.004	0.943	3.115	1.898
0.96	0.011	0.045	0.852	0.004	0.069	0.937	1.037	1.850
2.4	0.035	0.117	0.976	0.022	0.173	0.966	0.985	1.444

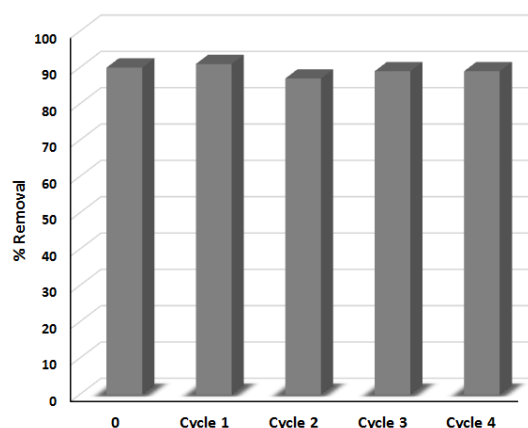


Figure 9: Removal of Pb(II) ions after various adsorption desorption cycles

Table 6
Comparison of Pb adsorption capacities of various biosorbents

Biosorbent	Q_m (mg/g)	Reference
Maize stover	19.65	[8]
Landoltia punctata	250	[15]
Spirodela plythiza	200	[15]
Cactus cladode	98.62	[9]
Sophora japonica pods	25.13	[51]
Citrus peels	480	[52]
Modified banana pseudostem	205.42	[53]
Modified sugarcane bagasse	116.7	[54]
Biochar	358.7	[55]
The present study	166	-

Regeneration study

Various methods have been investigated for the valorization of the loaded biomaterial in the literature, such as its regeneration, the use of the biosorbent as fertilizer for soils poor in essential microelements or the pyrolysis of exhausted biosorbents under well-defined conditions.³ In fact, to consider a biomaterial as an effective potential adsorbent for the removal of heavy metal ions, it should present not only an important adsorption capacity, but also good desorption of adsorbed molecules. Therefore, it appeared essential to examine the desorption of lead ions from the cactus biosorbent. The agent used for the desorption process was HCl at 0.1M. Several studies have shown that HCl is effective in desorbing heavy metals, when compared to other stripping agents, such as HNO₃, H₂SO₄ and NaOH.^{48,49} Desorption results for different cycles are shown in Figure 9.

As observed, the high percentage desorption of Pb(II) ions indicates the suitability of prickly pear cactus as a good potential adsorbent. Furthermore, the stability is an important parameter to be considered when the same adsorbent is re-used in multiple adsorption and desorption cycles. Therefore, the adsorption/desorption ability of the cactus biomaterial was investigated for four cycles of adsorption–desorption using 0.1 M HCl. It was observed that the adsorption of lead remained the same after the desorption step as the initial adsorption for the different cycles. This may be due to the effect of the acid agent during the desorption treatment, which can activate the pores of the adsorbent.⁵⁰ This finding indicates the stability of the cactus material and its suitability as a low-cost adsorbent for heavy metal removal.

Comparison of different biosorbents

The Pb adsorption capacity of the cactus cladode biomaterial used in this study was compared to those of other adsorbents developed in previous works, to highlight its efficiency compared to other materials reported in the literature. The corresponding biosorption capacities are summarized in Table 6. The adsorption retention of the used Tunisian cladode powder was found to be significant, compared to that of biosorbents. This can be explained by its various functional groups that can

exchange metal ions and can maintain high removal efficiency for many adsorption/desorption cycles. In addition, this material can be considered as a low-cost adsorbent, since it did not require any chemical or physical treatment to enhance its adsorption capacity. In fact, Tunisian dried cactus cladode, without any pretreatment, presents a maximum biosorption capacity of almost 166 mg/g for Pb(II), compared to many treated biosorbents. For example, Lacaran *et al.* achieved a Pb adsorption capacity of 205.42 mg/g by using nanofibrillated cellulose isolated from banana pseudostem and crosslinked with citric acid.⁵³ Liu *et al.* used citric acid- and Fe₃O₄-modified sugarcane bagasse (MSB) and reported an adsorption capacity of 116.7 mg/g.⁵⁴ Lian *et al.* produced biochar from an invasive plant by pyrolysis at 450 °C and obtained an adsorption capacity of 358.7 mg/g.⁵⁵

Thus, dried cactus cladode can be considered as an efficient, eco-friendly and low-cost biosorbent for the removal of heavy metals for industrial applications.

CONCLUSION

In this study, Tunisian cactus cladode was demonstrated to be a good adsorbent for lead removal from aqueous solution, with a removal capacity of almost 166 mg/g. The biosorbent's characterization results indicated the presence of widely distributed surface functional groups and good porosity, compared to other biomaterials.

The study of the effect of parameters, such as initial pH, temperature, initial concentration, particle size and stirring speed, on the adsorption process onto the developed cactus material, experiments were conducted. The solution pH was found to be the most important parameter influencing the adsorption, the percentage of lead removal increased from 34% to 80% when the pH was increased from 2.0 to 10. The adsorption equilibrium was fast, being achieved, under all conditions, after 120 min. Several models were used to fit equilibrium data. The adsorption isotherms were quite consistent with the Freundlich model for all experimental conditions (temperature and pH). The thermodynamic parameters indicated that the adsorption process is feasible and thermodynamically favored. The calculated adsorption energy proved the exothermic and chemical nature of the adsorption mechanism.

In the kinetic study, a high kinetic adsorption rate was achieved for the smaller particle size adsorbent (0.2-0.6 mm) and the highest stirring speed (500 rpm).

Fitting the experimental results to the different kinetic models revealed that the pseudo-second order model described best the biosorption kinetics. In order to distinguish the mechanism that controls the biosorption rate, the intraparticle diffusion model was applied, and film and pore diffusion coefficients were determined for different concentrations. The obtained results indicated that both intraparticle diffusion and film diffusion are the rate controlling steps of Pb(II) adsorption.

To prove the efficiency of cactus cladode as a low-cost adsorbent for heavy metals removal, regeneration tests were performed using an acidic solution. The findings revealed the regenerability and stability of the cactus cladode biosorbent, with about 87% removal capacity for four adsorption/desorption cycles.

Finally, the comparison of the adsorption capacity of the developed biosorbent with those of various other biomaterials reported in the literature proves its efficiency and suitability for heavy metals removal and wastewater treatment.

REFERENCES

- ¹ N. Genevois, N. Villandier, V. Chaleix, E. Poli, L. Jauberty *et al.*, *Ecol. Eng.*, **100**, 186 (2017), <https://doi.org/10.1016/j.ecoleng.2016.12.012>
- ² A. Esmaili and A. A. Beni, *Int. J. Environ. Sci. Technol.*, **12**, 2055 (2015), <https://doi.org/10.1007/s13762-014-0744-3>
- ³ I. S. Bădescu, D. Bulgariu, I. Ahmad and L. Bulgariu, *J. Environ. Manage.*, **224**, 288 (2018), <https://doi.org/10.1016/j.jenvman.2018.07.066>
- ⁴ J. Chen, Y. Tong, J. Xu, X. Liu, Y. Li *et al.*, *China Environ. Sci. Pollut. Rest. Int.*, **19**, 3268 (2012), <https://doi.org/10.1007/s11356-012-0837-9>
- ⁵ A. Aghababai and A. Esmaili, *Environ. Techn. Innov.*, **17**, 100503 (2020), <https://doi.org/10.1016/j.eti.2019.100503>
- ⁶ WHO Guidelines for Drinking-Water Quality, Geneva, 4th ed., World Health Organization, 2011, pp. 564
- ⁷ T. H. Derbe, *Chem. Mat. Eng.*, **5**, 15 (2017), <https://doi.org/10.13189/cme.2017.050201>
- ⁸ U. Guyo, J. Mhonyera and M. Moyo, *Process Saf. Environ. Prot.*, **93**, 192 (2014), <https://doi.org/10.1016/j.psep.2014.06.009>

- ⁹ N. Barka, M. Abdennouri, M. El Makhfouk and S. Qourzal, *J. Environ. Chem. Eng.*, **1**, 144 (2013), <http://dx.doi.org/10.1016/j.jece.2013.04.008>
- ¹⁰ M. M. A. A. El-Gendy and A. M. A. El-Bondkly, *Braz. J. Microbiol.*, **47**, 571 (2016), <https://doi.org/10.1016/j.bjm.2016.04.029>.
- ¹¹ A. Esmaeili and A. A. Beni, *Int. J. Environ. Sci. Technol.*, **15**, 765 (2018), <https://doi.org/10.1007/s13762-017-1409-9>
- ¹² R. M. Hlihor, H. Figueiredo, T. Tavares and M. Gavrilescu, *Process Saf. Environ. Prot.*, **108**, 44 (2017), <https://doi.org/10.1016/j.psep.2016.06.016>
- ¹³ T. A. Kurniawan, G. Y. S. Chan, W. Lo and S. Babel, *Sci. Total Environ.*, **366**, 409 (2006), <https://doi.org/10.1016/j.scitotenv.2005.10.001>
- ¹⁴ D. Purkayastha, U. Mishra and S. A. Biswas, *J. Water Process. Eng.*, **2**, 105 (2014), <https://doi.org/10.1016/j.jwpe.2014.05.009>
- ¹⁵ J. Tang, Y. Li, X. Wang and M. Daroch, *J. Clean. Prod.*, **145**, 25 (2017), <https://doi.org/10.1016/j.jclepro.2017.01.038>
- ¹⁶ P. Miretzky, C. Munoz and A. Carrillo-Chavez, *Bioresour. Technol.*, **99**, 1211 (2008), <https://doi.org/10.1016/j.biortech.2007.02.045>
- ¹⁷ A. E. Ofomaja, *Bioresour. Technol.*, **101**, 5868 (2010), <https://doi.org/10.1016/j.biortech.2010.03.033>
- ¹⁸ FAO, Agro-Industrial Utilization of Cactus Pear, Rome, 2013
- ¹⁹ T. Nharingo and M. Moyo, *J. Environ. Manage.*, **166**, 55 (2016), <https://doi.org/10.1016/j.jenvman.2015.10.005>
- ²⁰ Y. I. Abrha, H. O. Kye, Y. O. Jung and Y. E. Yoon, *Desalin. Water Treat.*, **12** 330 (2018), <https://doi.org/10.5004/dwt.2018.22309>
- ²¹ J. A. Fernandez-Lopez, J. M. Angosto and M. D. Avilés, *Sci. World J.*, **2014**, 1 (2014), <https://doi.org/10.1155/2014/670249>
- ²² A. Belayneh and W. Batu, *J. Water Resour. Ocean Sci.*, **4**, 18 (2015), <https://doi.org/10.11648/j.wros.20150401.13>
- ²³ T. Derbe, H. Dargo and W. Batu, *Chem. Mater. Res.*, **7**, 84 (2015)
- ²⁴ M. V. Lopez-Ramon, F. Stoeckli, C. Moreno-Castilla and F. Carrasco-Marin, *Carbon*, **37**, 1215 (1999), [https://doi.org/10.1016/S0008-6223\(98\)00317-0](https://doi.org/10.1016/S0008-6223(98)00317-0)
- ²⁵ G. A. Kovo, A. D. Folasegun and O. A. Kayode, *Alexandria Eng. J.*, **54**, 757 (2015), <https://doi.org/10.1016/j.aej.2015.03.025>
- ²⁶ A. Cleiton Nunes and M. C. Guerreiro, *Quim. Nova*, **34**, 472 (2011), <https://doi.org/10.1590/S0100-40422011000300020>
- ²⁷ I. Langmuir, *J. Am. Chem. Soc.*, **40**, 1361 (1918), <https://doi.org/10.1021/ja02242a004>
- ²⁸ S. Brunauer, P. H. Emmett and E. Teller, *J. Am. Chem. Soc.*, **60**, 309 (1938), <https://doi.org/10.1021/ja01269a023>
- ²⁹ H. Shang, Y. Lu, F. Zhao, C. Chao, B. Zhang *et al.*, *RSC Adv.*, **5**, 75728 (2015), <http://dx.doi.org/10.1039/C5RA12406A>
- ³⁰ V. Fontanier, V. Farines, J. Albet, S. Baig and J. Molinier, *J. Sci. Eng.*, **27**, 115 (2005), <https://doi.org/10.1080/01919510590925239>
- ³¹ J. Nawrockia and B. Kasprzyk-Hordern, *Appl. Catal. B*, **99**, 27 (2010), <https://doi.org/10.1016/j.apcatb.2010.06.033>
- ³² I. Louati, M. Fersi, B. Hadrich, B. Ghariani, M. Nasri *et al.*, *3Biotech*, **8**, 478 (2018), <https://doi.org/10.1007/s13205-018-1499-1>
- ³³ M. M. Dubinin and L. V. Radushkevich, *Proc. Acad. Sci. Phys. Chem. Sect.*, **55**, 331 (1947)
- ³⁴ O. Redlich and D. L. Peterson, *J. Phys. Chem.*, **63**, (1959), <https://doi.org/10.1021/j150576a611JPhysChem>
- ³⁵ Y. S. Ho, *Scientometrics*, **59**, 171 (2004), <https://doi.org/10.1023/B:SCIE.0000013305.99473.cf>
- ³⁶ Y. S. Ho and G. McKay, *Adsorption*, **5**, 409 (1999), <https://doi.org/10.1023/A:1008921002014>
- ³⁷ R. Sivaraj, C. Namasivayam and K. Kadirvelu, *Waste Manage.*, **21**, 105 (2001), [https://doi.org/10.1016/S0956-053X\(00\)00076-3](https://doi.org/10.1016/S0956-053X(00)00076-3)
- ³⁸ S. H. Chien and W. R. Clayton, *Soil Sci. Soc. Am. J.*, **44**, 265 (1980), <https://doi.org/10.2136/sssaj1980.03615995004400020013x>
- ³⁹ F. T. Li, H. Yang, Y. Zhao and R. Xu, *Chin. Chem. Lett.*, **18**, 325 (2007), <https://doi.org/10.1016/j.ccllet.2007.01.034>
- ⁴⁰ N. V. Farinella, G. D. Matos and M. A. Z. Arruda, *Bioresour. Technol.*, **98**, 1940 (2007), <https://doi.org/10.1016/j.biortech.2006.07.043>
- ⁴¹ J. V. Ibarra and R. Moliner, *J. Anal. Appl. Pyrol.*, **20**, 171 (1991), [https://doi.org/10.1016/0165-2370\(91\)80071-F](https://doi.org/10.1016/0165-2370(91)80071-F)
- ⁴² N. Barka, K. Ouzaouit, M. Abdennouri and M. Makhfouk, *J. Taiwan Inst. Chem. Eng.*, **44**, 52 (2013), <https://doi.org/10.1016/j.jtice.2012.09.007>

- ⁴³ H. N. Tran, S. J. You and H. P. Chao, *J. Environ. Chem. Eng.*, **4**, 2671 (2016), <http://dx.doi.org/10.1016/j.jece.2016.05.009>
- ⁴⁴ J. Febrianto, A. N. Kosasih, J. Sunarso, Y. Ju, N. Indraswati *et al.*, *J. Hazard. Mater.*, **162**, 616 (2009), <https://doi.org/10.1016/j.jhazmat.2008.06.042>
- ⁴⁵ W. J. Weber and J. C Morris, *J. Sanit. Eng. Div.*, **89**, 31 (1963), <https://doi.org/10.1061/JSEDAI.0000430>
- ⁴⁶ T. Bohli, A. Ouederni, N. Fiol and I. Villaescusa, *C. R. Chim.*, **18**, 88 (2015), <https://doi.org/10.1016/j.crci.2014.05.009>
- ⁴⁷ J. Crank, "The Mathematics of Diffusion", 2nd ed., Clarendon Press, Oxford, 1975, pp. 374
- ⁴⁸ R. K. Gautam, A. Mudhoo, G. Lofrano and M. G. Chattopadhyaya, *J. Environ. Chem. Eng.*, **2**, 239 (2014), <https://doi.org/10.1016/j.jece.2013.12.019>
- ⁴⁹ I. Smiciklas, S. Dimovic, I. Places and M. Mitric, *Water. Res.*, **40**, 2267 (2006), <https://doi.org/10.1016/j.watres.2006.04.031>.
- ⁵⁰ E. Igberase, P. Osifo and A. Ofomaja, *J. Environ. Chem. Eng.*, **2**, 362 (2014), <https://doi.org/10.1016/j.jece.2014.01.008>
- ⁵¹ W. A. R. Mohammad, A. Ahmad and A. M. Awwad, *Int. J. Ind. Chem.*, **6**, 67 (2015), <https://doi.org/10.1007/s40090-014-0030-8>
- ⁵² E. Njikam and S. Schiewer, *J. Hazard. Mater.*, **213/214**, 242 (2012), <https://doi.org/10.1016/j.jhazmat.2012.01.084>
- ⁵³ J. V. T. Lacaran, R. J. Narceda, J. A. V. Bilo and J. L. Leano, *Cellulose Chem. Technol.*, **55**, 403 (2021), <https://doi.org/10.35812/CelluloseChemTechnol.2021.55.38>
- ⁵⁴ G. Liu, L. Liao, Z. Dai, Q. Qi, J. Wu *et al.*, *Chem. Eng. J.*, **395**, 125108 (2020), <https://doi.org/10.1016/j.cej.2020.125108>
- ⁵⁵ W. Lian, L. Yang, S. Joseph, W. Shi, R. Bian *et al.*, *Bioresour. Technol.*, **317**, 124011 (2020), <https://doi.org/10.1016/j.biortech.2020.124011>